



A CONTRIBUTION TO THE MECHANISM OF “REDUCED” CO₂ ADSORBATES ELECTRO-OXIDATION FROM COMBINED SPECTROELECTROCHEMICAL AND VOLTAMMETRIC DATA

M. C. ARÉVALO,* C. GOMIS-BAS,* F. HAHN,† B. BEDEN,†† A. ARÉVALO* and A. J. ARVIAS§

* Departamento de Química-Física, Universidad de La Laguna, Av. Trinidad s/n, 38205 La Laguna, Tenerife, Spain.

† Université de Poitiers, Laboratoire de Chimie 1, URA CNRS 350, 40 Av. du recteur Pineau, 86022 Poitiers, France

§ Instituto de Investigaciones Físicoquímicas Teóricas y Aplicadas (INIFTA), Sucursal 4, Casilla de Correo 16, (1900) La Plata, Argentina

(Received 30 June 1993; in revised form 25 October 1993)

Abstract—The nature of reduced CO₂ adsorbates, as well as the mechanisms for their electro-oxidation on platinum, have been reviewed through the light of new experimental data obtained by cyclic voltammetry and by Fourier transform infrared reflectance spectroscopy. Three different “reduced” CO₂ adsorbates are described as “ensembles”. It is suggested that they involve different extents of adsorbed entities, among which weakly bound and strongly bound hydrogen atoms play the most important role.

Key words: spectroelectrochemistry, cyclic voltammetry, reduced CO₂, reflectance infrared spectroscopy, electrocatalysis.

INTRODUCTION

The adsorption of CO₂ on catalytic electrodes is favoured on H-adsorbing metals[1–7], as “reduced” CO₂ adsorbates formation requires interaction between CO₂ molecules and H-adatoms. These adsorbates play an important role as precursors in CO₂ electroreduction and also as probable reaction intermediates in the mechanism of electro-oxidation of simple organic molecules[1–7].

Electrochemical data concerning “reduced” CO₂ adsorbates electro-oxidation on Pt substrates indicate the possible formation of several CO₂ adsorbates and intraconversion reactions. It appears that the characteristics of “reduced” CO₂ adsorbates are closely related to the type of H-adatoms involved in their adsorption bonding to Pt[8–10].

Different “reduced” CO₂ adsorbates on Pt have been described as ensembles of CO₂, H and H₂O entities[8, 9], although it is not yet clear whether CO₂ exists in these ensembles either as such or as CO-type species. From EMIRS data of these species it was early recognised that adsorbed CO was one important species[11], although it was suggested that other species could contribute to “reduced” CO₂ adsorbates as well. SNIFTIRS experiments[12, 13] later confirmed the role of linearly bonded CO as a major species beside which bridge bonded CO and multi-bonded were also detected.

On the other hand, the possibility of intraconversion reactions[10] arises a number of questions

which are directly related to the electro-oxidation mechanism of adsorbed CO₂. As a matter of fact, the true “reduced” CO₂ adsorbed state, and its relation to weakly and strongly adsorbed H-atoms, the rate of the intraconversion processes, and the influence of potential perturbation, are still questions deserving further research.

This preliminary communication provides new spectroelectrochemical and voltammetric data which attempt to throw further light on the adsorbed CO₂ electro-oxidation mechanism, and to offer a bridge between those electro-oxidation and electroreduction processes involving CO₂ in aqueous solutions on H-adsorbing metals.

EXPERIMENTAL

The electrochemical measurements were performed in a flow electrochemical cell of about 50 ml capacity containing the usual three-electrode arrangement.

The experimental work was performed either on a polycrystalline (PC) Pt electrode or on a Pt electrode with a (100) preferred crystallographic orientation. This type of Pt surface, which is characterized by a relatively large density of surface sites for strongly bound H-atoms was prepared as reported in [14]. The counter electrode was a Pt electrode (geometric area ca. 1 cm²) mounted in a separate compartment. A Hg/Hg₂SO₄(s)/K₂SO₄(sat)/0.5 M H₂SO₄ reference electrode (*mse*) ($E/V(rhe) = 0.659$) was employed. Potentials in the text are referred to the *rhe* potential scale. The working electrode pretreatment consisted

† Author to whom correspondence should be addressed.

of a potential cycling in the 0.060–1.400 V range, at 0.200 V s^{-1} in $0.5 \text{ M H}_2\text{SO}_4$.

The base electrolyte solution was prepared from 98% sulfuric acid (Merck p.a.) and Millipore-MilliQ* water. CO_2 was prepared from the reaction between 50% H_2SO_4 and NaHCO_3 and bubbled through the solution. Runs were made at room temperature under either Ar or CO_2 saturation depending on the type of experiments.

Each run consisted of the following steps. Firstly, the voltammetric behaviour of H-atom electro-sorption reactions was followed under potential cycling at 0.2 V s^{-1} . The stability of these cyclic voltammograms was taken as a purity test of the system[15]. Then, the potential was stepped to E_{ad} the adsorption potential for CO_2 , and as the null current was attained at this potential, the solution was then saturated with CO_2 to form "reduced" CO_2 adsorbates. Subsequently, this solution was replaced by $0.5 \text{ M H}_2\text{SO}_4$ holding the potential at E_{ad} , and the proper voltammetric runs involving "reduced" adsorbates were performed.

The electrochemical set-up consisted of a PAR 173 potentiostat, PAR 179 automatic digital coulometer, PAR 175 Universal programmer, 3091 Nicolet digital oscilloscope and Yokogawa *x-y* recorder.

The Fourier transform infrared spectrometer was a Bruker IFS 66v, modified to allow the beam to reflect upon the *ir* window (CaF_2) of the conventional thin layer spectroelectrochemical cell with an incidence angle of 65° . All the beam path was under vacuum and the *ir* light was either *p*- or *s*-polarized according to the type of experiments. A N_2 cooled HgCdTe detector, from Infrared Associates, was used. Each spectrum resulted from the coaddition of 512 interferograms (acquisition time of about 20s). Spectral resolution was 8 cm^{-1} . Reference spectra

were taken as indicated in part 2 of the results section.

RESULTS

1. Voltammetric data

The adsorption of CO_2 on Pt in acids yielding "reduced" CO_2 adsorbates takes place in the H-atom electro-sorption potential range, and the voltammetric electro-oxidation of "reduced" CO_2 adsorbates in acids is characterized by a rather complex anodic peak extending from 0.6 to 0.9 V which partially overlaps the O-electro-adsorption current initial contribution. The adsorbed CO_2 electro-oxidation current peak actually consists of at least two largely overlapping anodic current peaks (Fig. 1), the relative contribution of which depends considerably on the adsorption potential (E_{ad}), the surface topography, the adsorption time (t_{ad}), the potential routine applied before running adsorbed CO_2 electro-oxidation and the solution composition[8, 9]. Runs made at $E_{\text{ad}} = 0.080 \text{ V}$ and $E_{\text{ad}} = 0.200 \text{ V}$ on PC and faceted Pt, covering the $0 \leq t_{\text{ad}} \leq 15 \text{ min}$ range in $0.5 \text{ M H}_2\text{SO}_4$ were made. Values of E_{ad} were chosen to assure two values of θ , the H-atom surface coverage degree, namely, $\theta(E_{\text{ad}} = 0.080 \text{ V}) \cong 1$ and $\theta(E_{\text{ad}} = 0.200 \text{ V}) \cong 0.5$ [10]. The influence of the different variables was demonstrated using several potential routines which are shown as insets together with the corresponding voltammograms (Fig. 1). From these experiments the following features were derived.

(i) For both Pt electrodes, the "reduced" CO_2 adsorbates electro-oxidation current peak is made of two main contributions which are denoted as peaks I and II. The appearance of these peaks can be taken

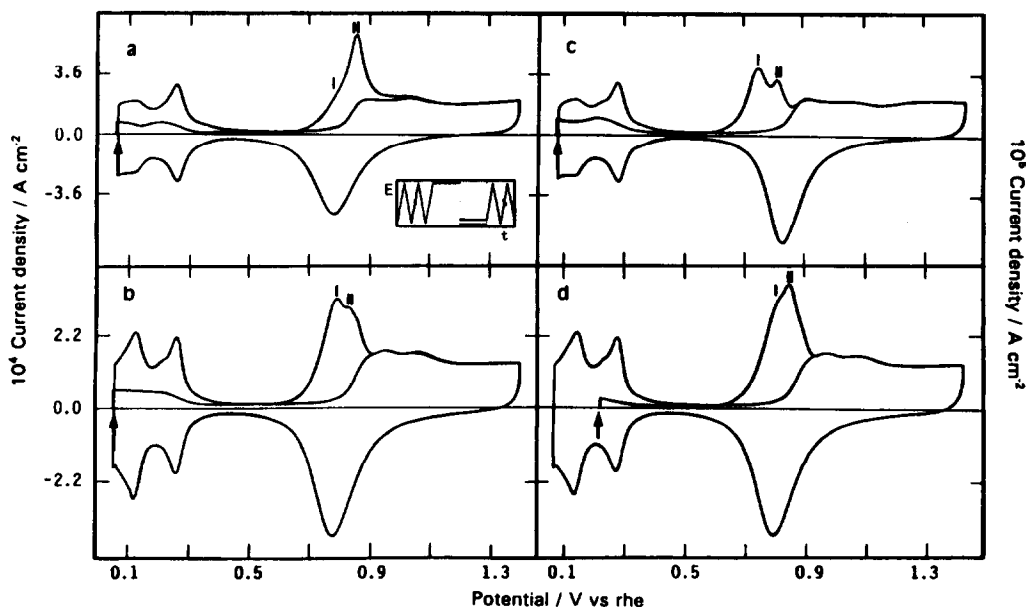


Fig. 1. Anodic stripping cyclovoltammograms of "reduced" CO_2 adsorbates in $0.5 \text{ M H}_2\text{SO}_4$: (a) (100) faceted Pt electrode, $v = 0.2 \text{ V s}^{-1}$, $E_{\text{ad}} = 0.08 \text{ V}$; (b) polycrystalline Pt electrode, $v = 0.2 \text{ V s}^{-1}$, $E_{\text{ad}} = 0.08 \text{ V}$; (c) (100) faceted Pt electrode, $v = 0.02 \text{ V s}^{-1}$, $E_{\text{ad}} = 0.08 \text{ V}$; (d) polycrystalline Pt, $v = 0.2 \text{ V s}^{-1}$, $E_{\text{ad}} = 0.2 \text{ V}$. Arrows indicate the E_{ad} values.

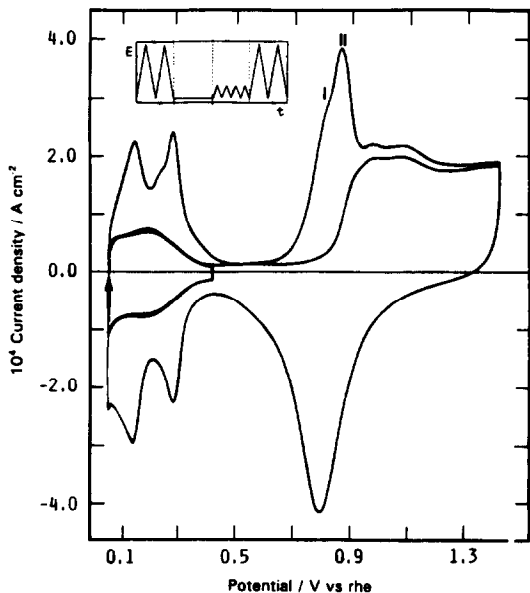


Fig. 2. Anodic stripping cyclic voltammograms of "reduced" CO₂ adsorbates in 0.5 M H₂SO₄; polycrystalline Pt electrode, $\nu = 0.2 \text{ V s}^{-1}$. Prior to the voltammetric run the working electrode was subjected to a potential cycling between 0.08 and 0.45 V at $\nu = 0.2 \text{ V s}^{-1}$.

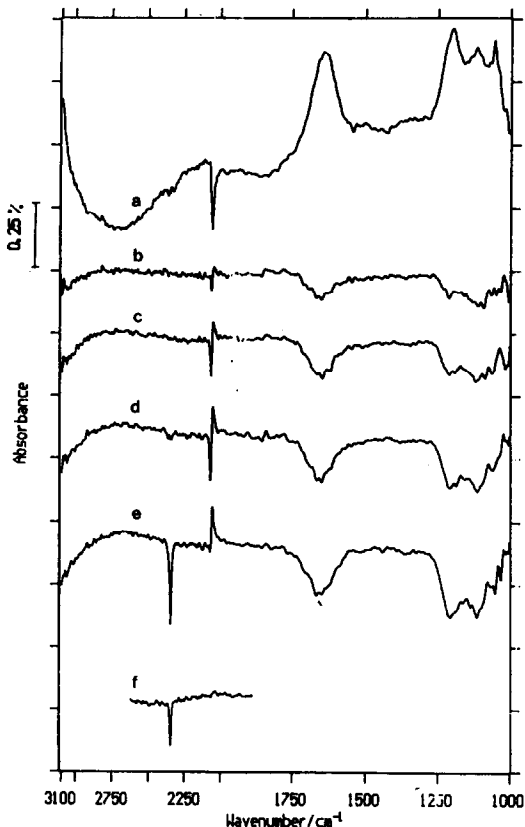


Fig. 3. SPAIRS at various potentials of the "reduced" CO₂ adsorbates at a polycrystalline platinum electrode in 0.5 M H₂SO₄. CO₂ was adsorbed at 0.2 V vs. (*rhe*). Polarization as follows: spectra (a)–(e) are *p*-polarized; spectrum (f) is *s*-polarized. Spectral subtraction as follows: (a) subtraction with Ref_A (see text). (b)–(f) subtraction with Ref_B. Potential as follows [after adsorption at 0.2 V vs. (*rhe*)]: (a) 0.3; (b) 0.3; (c) 0.4; (d) 0.5; (e) 0.6; (f) 0.6 V.

as a first indication of the formation of several "reduced" CO₂ adsorbates on Pt in aqueous acid solution at E_{ad} .

(ii) The peak I to peak II height ratio resulting from those runs made at constant E_{ad} , t_{ad} and ν , decreases in going from PC Pt to faceted Pt (Fig. 1, a and b). This change can be directly related to the θ_w/θ_s ratio for weakly (*w*) and strongly (*s*) bound H-adatoms already known for these electrodes[14, 16]. The height of peak II increases with θ .

(iii) For a given Pt substrate, those runs made at constant E_{ad} and t_{ad} , show that the peak I to peak II height ratio decreases as ν is increased, although the overall "reduced" CO₂ adsorbates electro-oxidation charge density remains practically constant. These results point out a possible restructuring or reaccommodation of adsorbates at the substrate surface (Fig. 1, a and c).

(iv) As E_{ad} is increased from $E_{ad} = 0.080$ to 0.200 V at constant t_{ad} , an increase in the contribution of peak II can be noticed, as if the formation of the most stable "reduced" CO₂ adsorbate was favoured at the most positive potential (Fig. 1, b and d).

(v) When the "reduced" CO₂ adsorbate electro-oxidation is preceded by a potential cycling of a few minutes duration in the H-adatoms potential range, an increase in the contribution of peak II can definitely be seen. This means that this potential cycling promotes also the stabilization of the most stable "reduced" CO₂ adsorbates (Fig. 2).

(vi) The maximum "reduced" CO₂ adsorbates electro-oxidation charge density is always about $0.20 \pm 0.02 \text{ mC cm}^{-2}$ irrespective of E_{ad} and anodic current peak multiplicity.

(vii) In all cases, the presence of CO₂ adsorbates leaves about 20% free sites on Pt for H-atom adsorption. The electrodesorption voltammogram of these H-adatoms differs appreciably from those of the blanks.

(viii) It is worth mentioning that the potential of peak II closely resembles that of the main CO adsorbate electro-oxidation current peak on PC Pt in acids for $\theta_{CO} \Rightarrow 1$ [17–19].

2. Spectroscopic data

Before each experiment, the purity of the spectroelectrochemical cell was tested. After that, at the adsorption potential for CO₂ (two adsorption potentials were chosen for this work: $E_{ads} = 0.08 \text{ V}$ and $E_{ads} = 0.2 \text{ V}$), the working electrode was pushed against the CaF₂ window and a first reference spectrum (Ref_A-type, reference without CO₂) was recorded. Then, CO₂ was introduced into the cell for 30 min, the electrode always being against the window and the potential still held at E_{ads} . For the complete elimination of dissolved CO₂, N₂ was bubbled for 30 min. A second reference spectrum (Ref_B-type, reference with CO₂) was recorded.

Then, using the so-called SPAIRS technique[20, 21], infrared reflectance spectra were taken at various electrode potentials, *ie* starting from E_{ads} , the potential was scanned positively at 0.5 mV s^{-1} and spectra were collected at 0.1 V steps. Two series of spectra were obtained by subtraction with the two types of references.

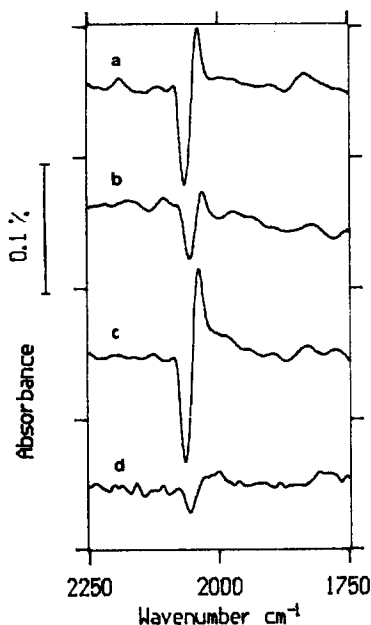


Fig. 4. SNIFTIRS of "reduced" CO_2 chemisorption at a polycrystalline platinum electrode in 0.5 M H_2SO_4 , *p*-polarization, potential modulation between (a) [0;300 mV/rhe]; (b) [100;400 mV/rhe]; (c) [200;500 mV/rhe] and (d) [300;600 mV/rhe].

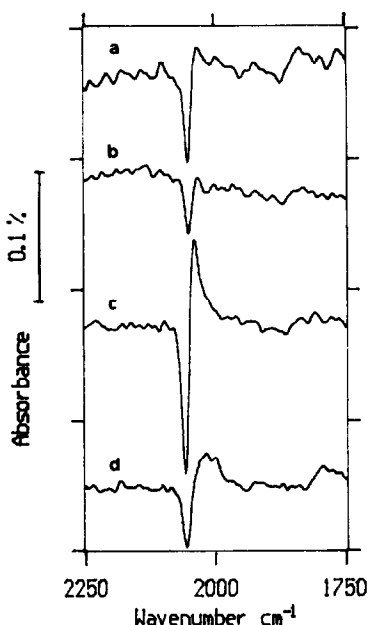


Fig. 6. SNIFTIRS of "reduced" CO_2 chemisorption at a (100) faceted platinum electrode in 0.5 M H_2SO_4 , *p*-polarization, potential modulation between (a) [0;300 mV/rhe]; (b) [100;400 mV/rhe]; (c) [200;500 mV/rhe] and (d) [300;600 mV/rhe].

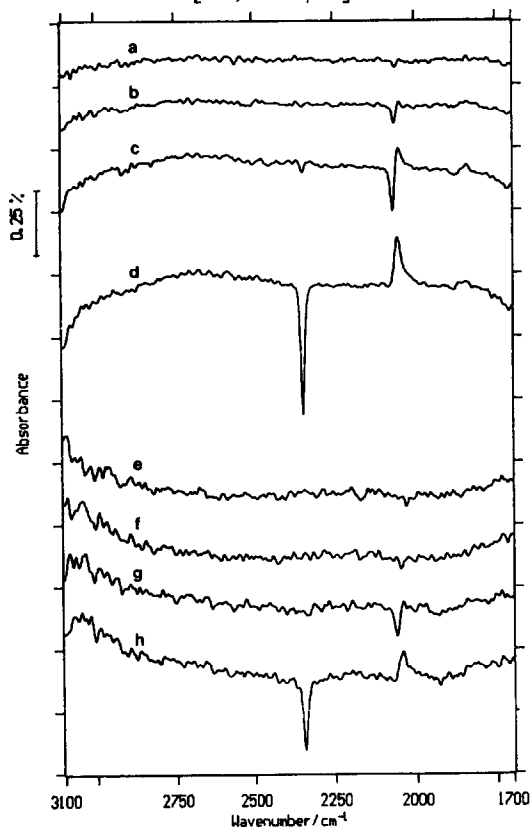


Fig. 5. SPAIRS of "reduced" CO_2 chemisorption in 0.5 M H_2SO_4 . Type of electrode surface: spectra (a)–(d), PC Pt; spectra (e)–(h) (100) faceted Pt. CO_2 was adsorbed at 0.08 V vs. (rhe). Reference for subtraction was of Ref_B type. Potential as follows [after adsorption at 0.08 V vs. (rhe)]: (a) and (e) 0.18 V; (b) and (f) 0.28 V; (c) and (g) 0.48 V; (d) and (h) 0.68 V.

Spectra a and b of Fig. 3, for $E_{ad} = 0.200$ V for PC Pt, emphasize well the importance of the choice of the reference spectrum. The subtraction with Ref_A (Fig. 3a) gives the state of the electrode surface immediately after the CO_2 adsorption. The negative band at 2050 cm^{-1} indicates the presence of linearly bonded CO, in agreement with previous EMIRS work [11, 22, 23], whereas the positive bands at ca. 1650 and $1250\text{--}1050\text{ cm}^{-1}$ show that water and sulphate-bisulphate anions [24–27] have been removed from the surface by more strongly adsorbed species. The subtraction with Ref_B (Fig. 3, spectra b–e) more clearly shows the influence of E_{ad} on the adsorbed layer. A derivative-like CO signal is seen when linearly bonded CO is present on the surface at the two potential limits (b, c and d). The linear CO band takes a single sided shape when the potential reaches 0.6 V (e). The last spectrum (f) is taken under the same conditions, but using a *s*-polarized infrared beam. The absence of the 2050 cm^{-1} band, as compared to spectrum (e), confirms its assignment to a surface species. Minor contribution from either multi bonded CO or bridge-bonded CO can be detected at 1850 and 1985 cm^{-1} , respectively (Fig. 4). The SNIFTIRS technique was used in that case because it is more suitable for detecting adsorbed species.

Figure 5 provides evidence about the different behaviours of polycrystalline Pt and faceted Pt for CO_2 electroreduction. At $E_{ad} = 0.080$ V (spectra a–d), the PC surface is partially covered by CO_{ad} species, as it was with $E_{ad} = 0.200$ V. The only difference being a slightly higher contribution of highly coordinated CO, shown by the small, but clear, band at ca. 1820 cm^{-1} . With faceted Pt (spectra e–h), the oxidation of CO_{ad} is delayed (*ie* it starts at higher potentials), a fact which is certainly related to the

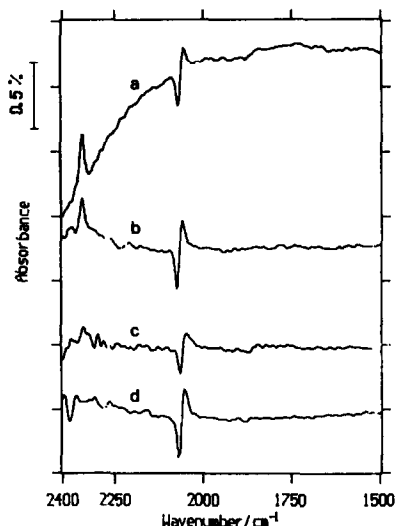


Fig. 7. SPAIRS obtained in D₂O of the "reduced" CO₂ adsorbates. (a) and (b) at a PC Pt electrode; (c) and (d) at a (100) faceted Pt electrode; (a) and (c) potential at 0.48 V after adsorption at 0.08 V vs. (*rhe*); (b) and (d) potential at 0.5 V after adsorption at 0.2 V vs. (*rhe*).

coexistence of a much larger proportion of highly coordinated CO. This is better seen when the SNIFTIRS technique is used (Fig. 6). The spectra clearly show the three adsorbed species, *ie* linearly bounded CO at 2042 cm⁻¹, bridge-bonded CO at 1937 cm⁻¹ and multi-bonded CO at 1855 cm⁻¹. Interestingly, these highly coordinated CO species are more present on faceted Pt than on polycrystalline Pt (Figs 4a and 6a). Although (100) faceted Pt does not behave exactly as a well-defined (100) surface, some similar features are observed. It is clear that the existence of highly coordinated CO depends both on the crystalline structure and on the electrode coverage, as it was already shown with gaseous CO[28] reduced CO₂[12] or methanol[29].

Similar experiments were also carried out in D₂O, to check whether the strong band at *ca.* 1650 cm⁻¹ was only due to water, or if carbonyl species (of aldehyde-type or acid-type) which would be formed upon CO₂ reduction could also contribute to its shape. The answer is quite clear from Fig. 7, neither with PC Pt (spectra a and b) nor with faceted Pt (spectra c and d) are bands detected in the 1600–1700 cm⁻¹ range.

DISCUSSION

The correlation of the electrochemical and spectroelectrochemical data can be made in terms of a reaction pathway involving as first stage the adsorption of CO₂ on H-atom covered sites yielding two distinguishable CO₂ adsorbates, whose properties depend on whether the CO₂ molecule is anchored by strongly bound H-adatoms (CO₂-adsorbate-I) or weakly bound H-adatoms (CO₂-adsorbate-II). CO₂-adsorbate-I undergoes a rather slow intraconversion reaction leading to an adsorbed ensemble (CO-adsorbate-III) consisting of CO directly bound to Pt, mainly under the linear form, surrounded by

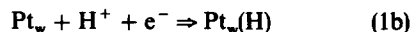
adsorbed OH, H-species and water molecules. According to this description the relative contribution of adsorbates I, II and III should depend considerably on *E*_{ad}, on the distribution of crystallographic faces at the substrate and on the potential routine. In any case, the relatively broad voltammetric peak at 0.8 V can be assigned to the electro-oxidation of adsorbate II, whereas the peak at 0.85 V can be related to the electro-oxidation of adsorbates I and III (Fig. 1a, b).

The *p*-polarized *ir* spectrum shows a maximum contribution of adsorbate-III when adsorbate-I is fully formed, *ie* for CO₂ adsorption at *E*_{ad} = 0.200 V. At this potential, no CO₂ signal at *ca.* 2345 cm⁻¹ can be observed in the spectrum, but when the potential is made more positive, the CO₂ signal appears as soon as the linear CO adsorbate band at 2050 cm⁻¹ begins to decrease.

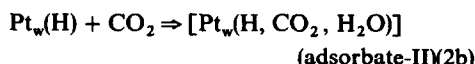
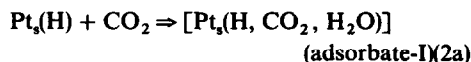
Otherwise, as the intensity of the CO₂ band exceeds that expected from the electro-oxidation of adsorbate-III, especially at short adsorption times, it appears that the CO₂ signal comes out from two different contributions, namely that from adsorbates I and II (by CO₂ release after H electro-oxidation) and that from adsorbate III (as a result of CO_{ad} oxidation). This can be understood if adsorbates I and II, which involve bondings with H-atoms, consist primarily of a O–C–O planar structure lying parallel to the substrate, thus being infrared inactive according to the surface relation rule. When CO₂ is released, it exhibits a sharp Q branch at 2345 cm⁻¹ in both *p*- and *s*-polarization states (Fig. 3, spectra e and f). But, the fact that no P and R branches are seen in the *p*-polarized spectra, whereas the two branches contribute weakly in the *s*-polarized spectra especially at high potentials is a clear indication of an adsorbed CO₂ species which enables the appearance of perpendicular band with the rotational relation rule $\Delta J = 0$.

On the other hand, the appearance of a CO-adsorbate III band at 2050 cm⁻¹ (and its intensity variation with potential) is accompanied by the appearance of related changes in hydroxyl bands, quite clear in D₂O solution, which are assigned to O–H bond vibration in the corresponding adsorbates III ensemble. The spectrum of adsorbate-III ensemble is then consistent with OH + CO coadsorbate structure on the substrate.

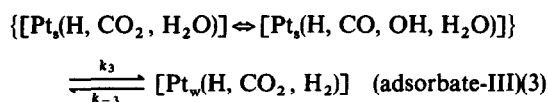
Based upon the preceding analysis, the initial stage of the CO₂ adsorption mechanism on Pt in acid is the H-adatom electroadsorption on Pt, which can be formally expressed as:



where parentheses stand for adsorbed species, and *s* and *w* denote Pt sites yielding strongly and weakly bound H-adatoms. Reactions (1a) and (1b) are followed by CO₂ attachment leading to the formation of adsorbed ensembles, without H-adatom release,

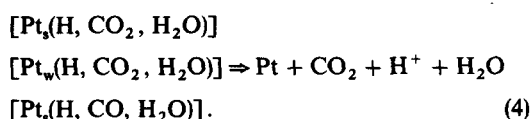


where brackets indicate adsorbate ensembles. Likewise, adsorbates I and II participate in a complex intraconversion process involving also a CO-containing ensemble (adsorbate-III) such as:



where the braces denote voltammetrically indistinguishable adsorbates I and III. The value of k_3 , the rate constant of reaction (3) in the forward direction at E_{ad} was estimated as 10^{-2} s^{-1} [30]. Therefore, the adsorption of CO_2 on Pt yields three different adsorbed species, their surface concentration ratio depending, in principle, on E_{ad} , t_{ad} , k_3 , surface concentration of s and w sites on Pt, *ie* on the distribution of crystallographic faces, and also on potential dependent competitive adsorption processes involving solution components, particularly anions [24–27].

On the other hand, the electro-oxidation of adsorbates I, II and III on both types of Pt electrodes should proceed through the formation of those CO_2 adsorbates which become infrared active to *p*-polarized *ir* light (Fig. 3). This means that in all cases, the overall electro-oxidation of CO_2 adsorbates yielding CO_2 and H^+ ion formation, can be expressed as a global process such as:



Overall reaction (4) gives rise to a multiplicity of anodic current peaks and to a maximum electro-oxidation charge density similar to that expected for the H-atom monolayer on PC Pt, *ie* 0.210 mC cm^{-2} .

In principle, reaction pathways (1–3) and (4) can be extended to Rh. However, as for this metal weak electroadsorbed H-atoms are predominantly formed, the contribution of adsorbate I would be considerably favoured over adsorbates II and III. Preliminary results obtained under the same experimental conditions, show that almost no adsorbed CO species are formed on this metal. Thus, spectroelectrochemical and voltammetric data resulting for both CO_2 adsorption and CO_2 adsorbates electro-oxidation on Rh in acid are fully consistent with the conclusions derived from the proposed reaction pathways.

In conclusion, the reaction pathways advanced for CO_2 adsorption and CO_2 adsorbates electro-oxidation on Pt in acids from spectroelectrochemical and voltammetric data accounts for:

(i) the influence of Pt substrate structure and history of the experiments on the formation of several CO_2 adsorbates;

(ii) the appearance of CO_2 and CO-containing adsorbed species on Pt and their relative contributions, which depend also on the substrate structure, the solution composition, and the history of the experiments;

(iii) the increase in the contribution of CO-containing adsorbate resulting either by increasing

t_{ad} at constant E_{ad} or by the potential cycling treatment in the H-atom electroadsorption potential range;

(iv) the main CO_2 adsorbates produced on Rh, a metal which presents a predominant contribution of weakly bound H-adatoms.

A more extended presentation of results and discussion of the aforementioned processes will be made in a forthcoming publication.

Acknowledgements—This work is being developed within the frame of the Acción Integrada Hispano-Francesa (1992) and the Programa de Cooperación Científica con Iberoamérica (1992) de los Ministerios de Educación y Ciencia y de Asuntos Exteriores of Spain.

REFERENCES

1. V. E. Kazarinov, V. N. Andreev and A. V. Shelepkov, *Electrochim. Acta* **34**, 905 (1989).
2. J. Giner, *Electrochim. Acta* **8**, 857 (1963).
3. M. W. Breiter, *Electrochim. Acta* **12**, 1213 (1967).
4. S. B. Brummer and M. J. Turner, *J. phys. Chem.* **71**, 3902 (1967).
5. B. I. Podlovchenko, V. F. Stenin and A. A. Ekibaeva, *Elektrokhimiya* **4**, 1004 (1968).
6. S. B. Brummer, K. Stenin and A. A. Ekibaeva, *Elektrokhimiya* **4**, 1004 (1968); **4**, 1374 (1968).
7. S. B. Brummer and K. Cahill, *J. electroanal. Chem.* **21**, 463 (1969).
8. M. L. Marcos, J. M. Vara, J. González-Velasco and A. J. Arvia, *J. electroanal. Chem.* **224**, 189 (1987).
9. M. L. Marcos, J. González-Velasco, J. M. Vara, M. C. Giordano and A. J. Arvia, *J. electroanal. Chem.* **281**, 257 (1990); **287**, 99 (1990).
10. M. C. Arévalo, C. Gomis-Bas, S. González, A. Arévalo and A. J. Arvia, Abstract 1-08, p. 142, 43rd ISE meeting, Córdoba (Argentina). 20–25 September (1992).
11. B. Beden, A. Bewick, M. Razaq and J. Weber, *J. electroanal. Chem.* **203**, 139 (1982).
12. B. Z. Nikolic, H. Huang, D. Gervasio, A. Lin, C. Fierro, R. R. Adzic and E. B. Yeager, *J. electroanal. Chem.* **295**, 415 (1990).
13. A. Aramata, M. Enyo, O. Koga and Y. Hori, *Chem. Letters C*, 749 (1991).
14. A. J. Arvia, J. C. Canullo, P. Custidiano, C. L. Perdiel and W. E. Triaca, *Electrochim. Acta* **31**, 1359 (1986).
15. B. E. Conway, H. Angerstein-Kozłowska, W. B. A. Sharp and E. E. Criddle, *Anal. Chem.* **45**, 1331 (1973).
16. A. T. Hubbard, R. M. Ishikawa and J. Katekaru, *J. electroanal. Chem.* **86**, 271 (1978).
17. E. P. M. Leiva, E. Santos, M. C. Giordano, R. M. Cerriño and A. J. Arvia, *J. electrochem. Soc.* **133**, 1660 (1986).
18. B. Beden, C. Lamy, N. R. de Tacconi and A. J. Arvia, *Electrochim. Acta* **35**, 691 (1990).
19. S. A. Bilmes, N. R. de Tacconi and A. J. Arvia, *J. electrochem. Soc.* **127**, 2184 (1980).
20. D. S. Corrigan, L. W. H. Leung and M. J. Weaver, *Anal. Chem.* **59**, 2252 (1987).
21. D. S. Corrigan and M. J. Weaver, *J. electroanal. Chem.* **241**, 143 (1988).
22. A. Bewick and B. S. Pons, in *Advances in Infrared and Raman Spectroscopy* (Edited by R. J. Clark and R. E. Hester), Vol. 32, Ch. 1. Wiley-Heyden, London.
23. B. Beden and C. Lamy, in *Spectroelectrochemistry, Theory and Practice*, (Edited by R. J. Gale), Plenum Press, New York (1988).
24. K. Kunimatsu, M. G. Samant and H. Seki, *J. electroanal. Chem.* **272**, 185 (1989).

25. P. W. Faguy, N. Markovic, R. R. Adzic, C. A. Fierro and E. B. Yeager, *J. electroanal. Chem.* **289**, 245 (1990).
26. F. C. Nart and T. Iwasita, *J. electroanal. Chem.* **308**, 277 (1991).
27. K. Kunimatsu, M. G. Samant and H. Seki, *J. electroanal. Chem.* **258**, 163 (1989).
28. S.-C. Chang and M. J. Weaver, *J. phys. Chem.* **94**, 5095 (1990).
29. S. Juanto, B. Beden, F. Hahn, J.-M. Léger and C. Lamy, *J. electroanal. Chem.* **237**, 119 (1987).
30. C. Gomis-Bas, forthcoming Thesis Doctoral, Universidad de La Laguna, Tenerife, Spain.